JOURNAL OF CATALYSIS 126, 401–420 (1990)

Temperature-Programmed Reaction of C_4 Oxygenates on Unpromoted and K-Promoted ZnCr Oxide in Relation to the Mechanism of the Higher Alcohol Synthesis*

LUCA LIETTI, PIO FORZATTI, ENRICO TRONCONI, AND ITALO PASQUON

Dipartimento di Chimica Industriale ed Ingegneria Chimica "G. Natta" del Politecnico, Piazza Leonardo da Vinci 32, 20133, Milano, Italy

Received April 18, 1989; revised January 25, 1990

The reaction mechanisms operating in the chain growth to C_{3+} primary alcohols and in the formation of ketones, secondary alcohols, methyl esters, ethers, and hydrocarbons during higher alcohol synthesis (HAS) over high-temperature modified methanol catalysts have been investigated by the temperature-programmed surface reaction (TPSR) technique. Experiments with linear and branched C_4 alcohols, aldehydes, and acids over an unpromoted ZnCr oxide sample have indicated a series of major catalyst functions, namely aldol-like condensation (also with oxygen retention reversal), decarboxylation and decarboxylative condensations, hydrogenation–dehydrogenation, dehydration and hydrolysis, along with isomerization and cracking. TPSR experiments with linear C_4 molecules over K-promoted ZnCr oxide have demonstrated the effects of alkali addition on the catalyst functions. The relevance of these functions and of the associated chemical reactions during HAS has been discussed in the light of catalytic tests performed under real synthesis conditions. The results are supportive of a mechanism of chain growth to C_{3+} primary alcohols based on a sequence of aldolic condensations of aldehydes, which do not operate over 2-methyl species. Formation of ketones under TPSR conditions is explained by decarboxylative condensation reactions of aldehydic and carboxylate species, as well as by aldol-like condensation reactions with oxygen retention reversal. Secondary alcohols detected in the products of the synthesis are formed by hydrogenation of ketones. Methyl esters and ethers are produced in the synthesis by alcoholysis of carboxylate and alkoxide species, respectively. Decarboxylation of carboxylate species, along with dehydration, may also play a role in the formation of hydrocarbons during HAS.

INTRODUCTION

Although much work has been devoted to the study of the direct synthesis of mixtures of methanol and higher alcohols (higher alcohol synthesis, HAS) over alkali-promoted methanol catalysts (*1–14*), some aspects of the synthesis have not yet been completely clarified.

A number of mechanistic proposals have been recently advanced to describe the origin of oxygenated products over modified Cu-based low-temperature methanol catalysts. In a series of exhaustive studies on the synthesis of oxygenates from syngas, Klier and co-workers (*15–18*), mainly on the basis of isotopic labelling experiments over Cs-promoted Cu/ZnO catalysts proposed that: (i) methyl formate originates from the direct carbonylation of a methoxy species; (ii) the C–C bond in ethanol is formed by coupling of C_1 surface intermediates related to methanol; (iii) carbon chain growth to C_{2+} oxygenates occurs by addition of oxygenated species at the β-carbon atom of the growing intermediate, both with classic aldol coupling and with aldol coupling with

*Paper XXI in the series "Synthesis of Alcohols from Carbon Oxides and Hydrogen."

0021-9517/90 $3.00

oxygen retention reversal; and (iv) this latter mode is specific to the presence of alkali and is responsible for the formation of ketones and for the higher productivity to propanol. Similar conclusions have been almost simultaneously reached by Elliott and Pennella (*19–22*) on the basis of isotopic labelling studies under HAS conditions over a Cu/ZnO methanol catalyst and of direct observation of the reaction products in microreactor experiments.

Concerning the high-T-modified methanol catalysts, mechanistic aspects of HAS were investigated in the early literature. Frolich and Cryder (*23*) and Graves (*24*) ascribed the formation of higher alcohols to the condensation of lower alcohols. Morgan (*25, 26*) described the formation of alcohols through a series of aldol condensation reactions starting with formaldehyde condensing to glycolaldehyde and proceeding through successive condensation, dehydration, and hydrogenation reactions to higher alcohols. Natta *et al.* (*7*) proposed a series of reactions involving CO insertion into an alkali alkoxide species to give the next higher carboxylate which is then reduced to alcohol. More recently Riva *et al.* (*8*) performed experiments with K-promoted ZnCr oxide catalysts where C_1 and C_2 oxygenates were added to the synthesis gas mixture; the results were found to be consistent with the hypothesis that chain growth takes place through insertion of a C_1 unit in the β-position of a C_n unit. A kinetic model for the distribution of C_{2+} primary alcohols has been recently reported for HAS over a Cs_2O-promoted ZnCr oxide catalyst (*27*). The related reaction scheme was based on two dominant pathways: (a) the stepwise C_1 addition to a growing linear chain; (b) a faster "β-condensation" route, leading to 2-methyl-branched alcohols. All of the above schemes are consistent with a chain growth mechanism based on a first slow step, responsible for the formation of the first carbon–carbon bond, followed by a fast chain growth leading primarily to branched primary alcohols.

The formation of minor amounts of ketones and of the corresponding secondary alcohols was explained by Natta *et al.* (*7*) through decomposition of alkali salts of fatty acids. The formation of hydrocarbons among the reaction products, although of great relevance for process implications, has not been specifically addressed so far. It is worth stressing that all of the above mechanistic proposals for HAS over alkali-promoted high-T-methanol catalysts rely mainly on qualitative analysis of the reaction product mixture, whereas direct evidence for their relevance is still lacking.

The present paper reports results of a study on the mechanisms involved in the alcohol chain growth and in the origin of side products such as ketones, secondary alcohols, esters, ethers, and hydrocarbons during HAS over an unpromoted and a K-promoted ZnCr oxide catalyst. The mechanism of HAS has been addressed by using the temperature programmed surface reaction (TPSR) technique, which allows one to collect valuable information on the surface reaction mechanism through the analysis of the desorption spectra of the products originating from decomposition or reaction of the adsorbates on the catalyst surface. By focusing attention on the interaction of appropriate intermediate species with the catalyst, this technique allows one to study the mechanism of specific reactions operating in HAS, and also reduces the complexity associated with the large number of reaction products.

In previous papers the interaction of *n*-butanal and 1-butanol with a ZnCr oxide catalyst has been investigated by the same technique (*28, 29*). A variety of desorption products that were considered to originate from C_4 and C_8 intermediate surface species were identified, and a number of chemical functions of the ZnCr oxide were pointed out. In this work the desorption spectra of *n*-butanal and 1-butanol have been recorded again in a TPSR apparatus which has been improved in order to obtain complete desorption traces for all products: they are presented here in a more complete form than previously reported

and discussed briefly for the sake of comparison. The TPSR study over unpromoted ZnCr oxide has been extended to *n*-butanoic acid, and to isobutanol, isobutanal and isobutanoic acid. The TPSR study of *n*-butanoic acid has been undertaken with the purpose of obtaining direct information on the reactivity of carboxylate ions. The TPSR study of branched C_4 oxygenated molecules was expected to confirm the catalyst functions previously assessed in the case of linear C_4 molecules, to provide evidence for additional functions due to the different reactivity of branched molecules as compared to the corresponding linear ones, and to give information on the terminal nature of branched C_4 alcohols and aldehydes in the HAS chain growth.

In this paper we also report on TPSR experiments of 1-butanol, *n*-butanal, and *n*-butanoic acid on K_2O-promoted ZnCr oxide; these have been performed to investigate the effect of alkali addition on the chemical functions of the ZnCr oxide system.

Finally, the role of the catalyst functions and the relevance of the associated chemical reactions under HAS conditions is discussed in the light of information provided by catalytic tests performed under real synthesis conditions.

METHODS

The TPSR apparatus, the related experimental procedures, and the GC–FTIR facilities have been described in detail elsewhere (*29*). For the present study, the analysis section of the TPSR apparatus has been enhanced by including a 16-loop gas sampling valve, which allowed several on-line GC analyses of the gas exiting the reactor to be performed during a single TPSR experiment, and by using an OV1 25-m-long capillary column (0.32-mm i.d.) with high phase thickness (3 μm) for the on-line GC analysis of both light and heavy desorbed products. The heating program for the GC analysis was typically 5 min at 30°C, followed by heating to 90°C (heating rate 5°C/min) and then to 230°C (heating rate 9°C/min, hold 10 min). The capillary column was coupled with a Poropak packed column (i.d. = 4 mm, L = 2 m) operating at 120°C, which enabled TC detection of species not monitored by FID (e.g., CO_2).

The desorption profiles of the single species were obtained by staged interpolation of the discrete experimental points, using cubic spline functions. No attempts were made to check the carbon balance, but the analysis of the catalyst after the TPSR run indicated that fouling occurred to a limited extent during the experiments, as discussed in (*29*).

A commercial ZnCr oxide catalyst with Zn/Cr atomic ratio 3/1 and BET surface area 120 m^2g^{-1} has been used in this study. XRD analysis indicated the presence of both ZnO and $ZnCr_2O_4$ phases. The K_2O-promoted sample (3% K_2O w/w) was obtained by the wet impregnation method using a CH_3COOK solution. The K loading corresponds to that typically used in HAS (*9*). The samples were prereduced with a N_2 + 5% H_2 mixture at 450°C for 30 min, saturated with the selected oxygenated molecules at 35°C and then evacuated to remove the weakly physisorbed species before recording the TPSR spectra. The TPSR experiment differs from a typical TPD experiment in that the desorbed species are not produced by simple desorption of the initially adsorbed molecules but originate from either surface-catalyzed decomposition of the adsorbate or from reaction between adsorbate in an inert carrier.

Zinc *n*-butyrate and zinc isobutyrate used as standards were prepared by attack on $ZnCO_3$ with butanoic acids at room temperature (r.t.). The IR spectra were recorded on a Perkin Elmer Model 782 instrument. Chromatographic helium, further purified by molecular sieves, and Fluka p.p.a. reagents were used during all runs.

RESULTS AND DISCUSSION

(a) Adsorption of Linear C_4 Oxygenated Molecules on Unpromoted ZnCr Oxide

1. 1-Butanol TPSR on ZnCr Oxide

The overall FID–TPSR trace and the profiles of the main desorbed species upon 1-

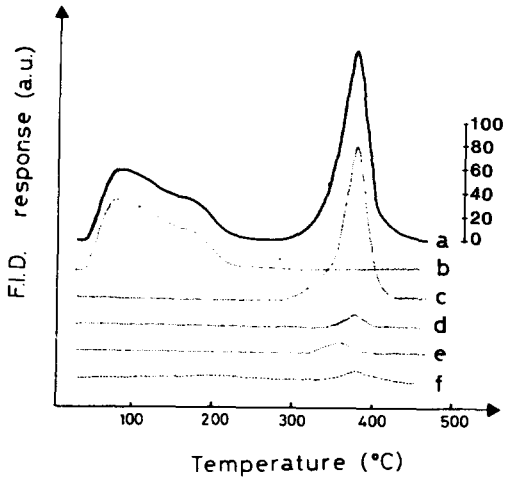

FIG. 1. FID–TPSR traces obtained after 1-butanol adsorption at 35°C on ZnCr oxide. (a) Overall FID–TPSR trace; (b) 1-butanol; (c) propylene; (d) butenes; (e) C_5 hydrocarbons; (f) methane + ethylene. The scale on the right is given for purposes of comparison with the TPSR traces presented in the following figures.

butanol adsorption on ZnCr oxide are shown in Fig. 1. Two main peaks are evident in the overall trace: a low temperature peak associated with the desorption of 1-butanol (with traces of *n*-butanal) and a high-temperature peak primarily associated with the evolution of propylene. Minor amounts of butenes, methane, ethylene, and C_5 hydrocarbons, and traces of C_5 and C_7 ketones (not reported in the figure) were also monitored. The data obtained using a TC detector showed the presence of CO_2 in the temperature region corresponding to propylene evolution.

2. *n-Butanal TPSR on ZnCr Oxide*

Figure 2 presents the FID–TPSR spectra obtained after a saturation dose of *n*-butanal on the ZnCr oxide catalyst. The most abundant products in the low-temperature region are 2-ethyl-2-hexenal, *n*-butanal, 1-butanol, and 4-heptanone. C_8 dienes (two isomers) are responsible for the weak maximum at 250°C. C_7 linear olefins (all five possible isomers), propylene, butenes, and 4-heptanone together with traces of methane, ethylene, C_5 hydrocarbons, C_7 dienes, toluene, and C_8 ketones (two isomers) comprise the composite high-temperature peak. C_7 linear olefines and propylene are primarily responsible for the shoulder at ≈350°C and for the maximum at 380°C, respectively. The data obtained using a TC detector revealed the presence of CO_2 in the high-temperature region.

3. *n-Butanoic Acid TPSR on ZnCr Oxide*

The desorption spectra recorded upon heating the ZnCr oxide sample, previously saturated with *n*-butanoic acid, are shown in Fig. 3. In the low-temperature region (below 250°C) the only species detected is the parent molecule, *n*-butanoic acid. Its desorption trace presents a shoulder at $T \approx 100$°C and a maximum at $T_M \approx 230$°C. White solid

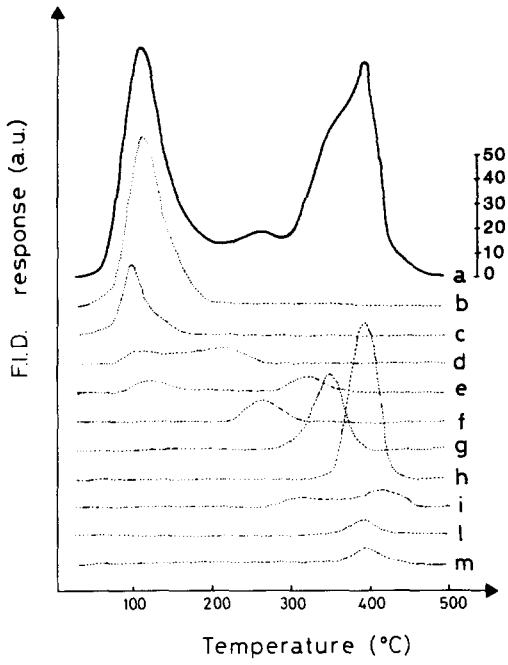

FIG. 2. FID–TPSR traces obtained after *n*-butanal adsorption at 35°C on ZnCr oxide. (a) Overall FID–TPSR trace; (b) 2-ethyl-2-hexenal; (c) *n*-butanal; (d) 1-butanol; (e) 4-heptanone; (f) C_8 dienes; (g) C_7 linear olefins; (h) propylene; (i) butenes; (l) C_5 hydrocarbons; (m) methane + ethylene.

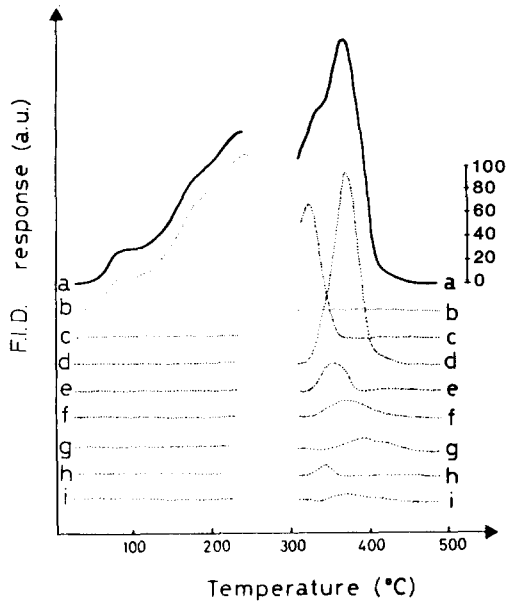

FIG. 3. FID–TPSR traces obtained after *n*-butanoic acid adsorption at 35°C on ZnCr oxide. (a) Overall FID–TPSR trace; (b) *n*-butanoic acid, (c) 4-heptanone, (d) propylene; (e) C_5 hydrocarbons; (f)) methane + ethylene; (g) butenes; (h) 2-pentanone; (i) toluene.

particles were observed in the carrier gas exiting the reactor in the temperature range 250–320°C, which prevented quantitative on-line analysis of the desorbed species. Accordingly their TPSR traces are not reported in this range. However, the condensed product was analyzed by HRGC: it was mainly constituted by *n*-butanoic acid and 4-heptanone. The IR spectrum of the solid corresponds to that of zinc *n*-butyrate, which can be formed via the etching of Zn from the catalyst by *n*-butanoic acid. The evolution of metal Zn at high temperature was observed by Vohs and Barteau (*30, 31*) during TPD of acetic acid, acetaldehyde, propionic acid, and propionaldehyde from the (0001) Zn surface of ZnO.

The main species detected in the TPSR products above 320°C are 4-heptanone ($T_M \approx 330$°C) and propylene ($T_M \approx 380$°C). The minor species include C_1–C_5 hydrocarbons (methane, ethylene, butenes, pentenes), aromatics (benzene and toluene), and 2-pentanone; their relative amounts increase with increasing temperature. By using a TC detector, the desorption of CO_2 could be monitored in the region corresponding to the high-temperature peak.

4. *Origin of C_4 Intermediate Surface Species and Desorbed Products*

A comprehensive mechanism representing the interaction of the C_4 oxygenated compounds with the ZnCr oxide surface is outlined below. Figure 4 shows the proposed C_4 intermediate surface species formed upon adsorption of 1-butanol, *n*-butanal, and *n*-butanoic acid ($R = -CH_2CH_2CH_3$) on the ZnCr oxide sample, and the species desorbed therefrom.

The existence of some of the proposed surface species and their stability with temperature have been recently determined by transmittance IR spectroscopy experiments on ZnO upon adsorption of 1-butanol, *n*-butanal, and *n*-butanoic acid (*32*). The commercial ZnCr oxide catalyst was not used since its excessive particle size prevented transmittance of IR experiments. However, a diffuse reflectance IR (DRIFT) spectrum of *n*-butanal adsorbed on this sample at r.t. was found to be quite consistent with the corresponding transmittance spectrum recorded on ZnO, confirming that the IR measurements on ZnO are representative of the situation on the surface of ZnCr oxide as well.

Molecularly adsorbed species. Species A_1, A_3, and A_6 represent the molecularly coordinated alcohol, aldehyde, and acid, respectively. They are formed upon adsorption at room temperature (routes I) of the gaseous molecules:

$$C_4H_9OH_{(g)} \rightleftharpoons C_4H_9OH_{(a)} \quad (1)$$

$$C_3H_7CHO_{(g)} \rightleftharpoons C_3H_7CHO_{(a)} \quad (2)$$

$$C_3H_7COOH_{(g)} \rightleftharpoons C_3H_7COOH_{(a)}. \quad (3)$$

The reverse of reactions (1), (2), and (3) (routes II) account for alcohol, aldehyde, and acid desorption with $T_M = 80$, 78, and

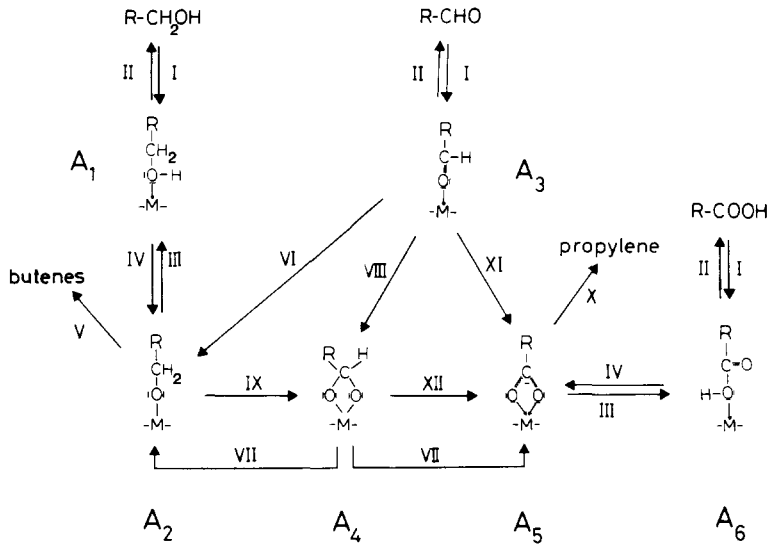

FIG. 4. Proposed reaction mechanism involving C_4 intermediate surface species and products desorbed therefrom. The bars beside the oxygen atoms correspond to a lone pair of electrons.

100°C (shoulder) in the corresponding TPSR spectra.

Alkoxide species. The alkoxide surface species A_2 of Fig. 4 originates from alcohol dissociative adsorption (route I + route IV) (*33*):

$$O_{(s)} + C_4H_9OH_{(a)} \rightarrow C_4H_9O_{(a)} + OH_{(a)}. \quad (4)$$

Hydrolysis of species A_2 (route III) followed by desorption results in the evolution of 1-butanol above T_M = 100°C in 1-butanol TPSR; this eventually accounts for the broad composite shape of the low-temperature peak. Dehydration of the alkoxide species A_2 (route V) leads to the desorption of butenes in correspondence to the high-temperature peak. The FTIR investigation (*32*) has shown the existence of alkoxide species following adsorption of 1-butanol on ZnO. Such species desorbed or decomposed between r.t. and 200°C. The same species A_2 are likely to be present during *n*-butanal TPSR as well, since 1-butanol and butenes are detected among desorbed products in the same temperature regions seen during 1-butanol TPSR. In this case species A_2 can be formed via reduction of the molecularly adsorbed aldehyde by hydrogen adsorbed during catalyst pretreatment (route VI) or via a Cannizzaro-type disproportionation reaction (route VII). Indeed, the formation of a dioxybutylidene species (route VIII) which acts as intermediate in the Cannizzaro-type disporportionation reaction (species A_4 of Fig. 4) has been indicated by FTIR upon *n*-butanal adsorption at r.t. on both ZnO and ZnCr oxide (*32*).

Carboxylate species. The carboxylate ion A_5 is formed upon *n*-butanoic acid dissociative adsorption (*33, 34*) (route I + route IV):

$$O_{(s)} + C_3H_7COOH_{(a)} \rightarrow C_3H_7COO_{(a)} + OH_{(a)}. \quad (5)$$

Hydrolysis of species A_5 (route III) followed by desorption results in the evolution of *n*-butanoic acid at $T > 100$°C in *n*-butanoic acid TPSR. The same species A_5 undergoes a selective decarboxylation reaction at higher temperatures (route X), leading to the evolution of propylene + CO_2 (T_M = 380°C):

$$CH_3CH_2CH_2COO_{(a)} \rightarrow C_3H_{6(g)} + CO_{2(g)} + H_{(a)}. \quad (6)$$

The formation of carboxylate species upon acid adsorption on oxide surfaces is well known. Vohs and Barteau have published XPS and UPS evidence that surface acetate species are formed following acetic acid adsorption on the Zn polar surface of zinc oxide (*30*). These authors conclude that the same surface species are formed also upon adsorption of acetaldehyde based on the similarity of the TPD spectra recorded with the two reactants.

Carboxylate species have also been detected by FTIR upon *n*-butanal and 1-butanol adsorption on ZnO (*32*). Such species were found to be stable under FTIR conditions up to 300–365°C. Indeed, the evolution of propylene + CO_2 is evident at the same temperature (T_M = 380°C) in *n*-butanoic acid, 1-butanol, and *n*-butanal TPSR. This fact provides a direct proof that the carboxylate ion A_5 is present during alcohol and aldehyde TPSR as well. The carboxylate ion can be formed from the molecularly adsorbed aldehyde (A_3) already at r.t. via oxidation by lattice oxygen (route XI in Fig. 4) or via a Cannizzaro-type disproportionation reaction involving the dioxybutylidene species A_4 (route VII), and from the alkoxide species (A_2) again via oxidation at temperatures above r.t. (*32*) (route IX + XII). In addition, for both aldehyde and alcohol molecules, an alternative route involving coadsorbed water or hydroxylate species cannot be ruled out. FTIR showed that between r.t.and 200°C alkoxide species originating from 1-butanol adsorption on ZnO give rise to carboxylate species which disappear again between 300 and 365°C. The presence on oxide surfaces of strongly bonded carboxylate groups, which decompose only at high temperatures, was already suggested in the case of adsorption of aldehydes (*35, 36*) and alcohols (*37, 38*).

Different amounts of propylene have been detected upon heating in 1-butanol, *n*-butanal, and *n*-butanoic acid TPSR (see Figs. 1, 2, and 3). This indicates that the coverage of the carboxylate species was different in each case; however, no coverage-dependence of the peak temperature was observed, which is typical of first-order desorption kinetics (*39*). Accordingly propylene + CO_2 desorption occurs via the decomposition reaction (6) with first-order kinetics in the surface coverage of the carboxylate ion A_5. For a first-order decomposition process, the following equation can be used to estimate the activation energy E_d of decomposition (*39*):

$$E_d/RT_M^2 = (k^\circ/\beta)\exp(-E_d/RT_M), \qquad (7)$$

where R is the gas constant, T_M is the peak maximum temperature, k° is the preexponential factor, and β is the heating rate. In the following, the usual value of normal vibrational frequency, that is 10^{13} s^{-1}, is assigned to k°. For the carboxylate ion, a value of E_d = 44.9 kcal/mol has been estimated from the peak temperature for β = 10.5°C/min.

5. *Origin of C_8 Intermediate Surface Species and Desorbed Products*

The presence of surface C_8 precursors was already suggested to account for the desorption of C_8 and C_7 products in *n*-butanal TPSR (*29*). Furthermore, results of FTIR experiments of *n*-butanal and *n*-butanoic acid adsorption (*32*) are consistent with the presence of C_8 aldehydic and carboxylate intermediate surface species on the catalyst surface. The splitting of the ν(C = O) band observed by IR after *n*-butanal adsorption has been attributed to the copresence of chemisorbed aldehydic species related to *n*-butanal and 2-ethyl-2-hexenal. IR after *n*-butanal and *n*-butanoic acid adsorption has also indicated the presence of two distinct forms of carboxylate species: the former, more resistent to heat treatment, is identified as species A_5 in Fig. 4, associated with propylene evolution; the latter is enhanced by prolonged contact time with vapors of *n*-butanal, decomposes at lower temperature, and is identified as species B_3 or B_4 in Fig. 5. A reaction pattern involving the C_8 surface intermediates can then be depicted as in Fig. 5.

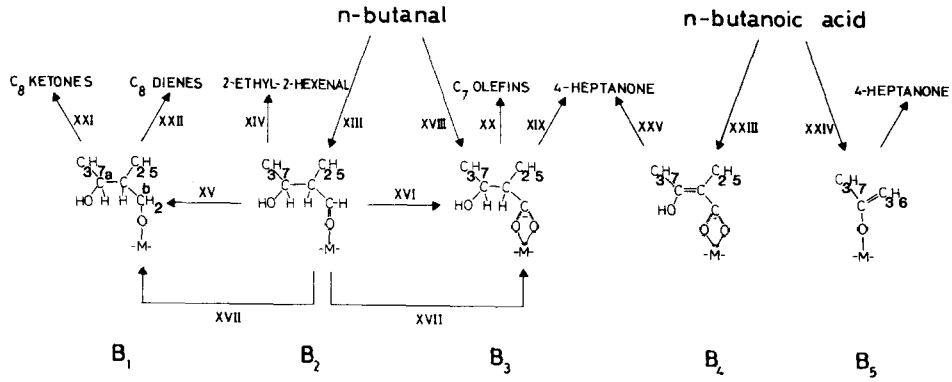

FIG. 5. Proposed reaction mechanism involving C_8 intermediate surface species formed upon *n*-butanal and *n*-butanoic acid adsorption and products desorbed therefrom. Symbols as in Fig. 4.

C_8 intermediate surface species during n-butanal TPSR. Species B_2 originates from aldol-like condensation of two *n*-butanal molecules (route XIII). Dehydration of this species (route XIV) leads to 2-ethyl-2-hexenal. The aldol condensation reaction occurs during adsorption at 35°C, since 2-ethyl-2-hexenal is detected in the gas exiting the reactor during *n*-butanal adsorption.

As already discussed for species A_3, in addition to the molecularly adsorbed species, the corresponding alkoxide and carboxylate species B_1 and B_3 are likely to be present. Their formation could involve either reduction (route XV) and oxidation (route XVI) reactions of the molecularly adsorbed species B_2, respectively, or a Cannizzaro-type disproportionation of the same species (route XVII). Species B_3 may also be formed via reaction of a surface C_4 carboxylate species with a neighboring molecularly adsorbed *n*-butanal molecule (route XVIII). Such a mechanism has been proposed for the condensation of carboxylic acids with carbonyl compounds on oxide surfaces (*40*). Dehydrogenation, decarboxylation, and keto-enol tautomerism of species B_3 gives rise to 4-heptanone (route XIX), whereas dehydration–decarboxylation of the same species leads to the desorption of C_7 linear olefins (route XX).

Species B_1 is involved in the desorption of C_8 ketones and C_8 dienes. These products result from dehydration on a C^b carbon atom, followed by double bond migration and keto-enol tautomerism (route XXI) and by dehydration on both C^a and C^b carbon atoms (route XXII), respectively (*29*). The formation of C_8 ketones implies an aldol-like condensation reaction with oxygen retention reversal. As shown in Fig. 6, such a mechanism is based on the retention of the anionic oxygen and on the hydrogenation of the –CHO group in the aldol intermediate (I) formed upon condensation of two aldehydic molecules. Evidence for a similar mechanism on a Cu-based catalyst under HAS conditions has recently been collected by using labelled C_1 molecules (*18*) as well as upon reaction of linear primary alcohols (including 1-butanol) over $CuO/ZnO/Al_2O_3$ (*21*).

The presence of an adsorbed 2-ethyl-2-hexenal molecule originating from dehydration of species B_2 and of the corresponding alkoxide and carboxylate species cannot be ruled out. These species may provide alternative routes to the desorption of C_8 dienes and C_7 linear olefins as depicted in Fig. 7. In order to test the feasibility of such routes, a TPSR experiment where 2-ethyl-2-hexenal was preadsorbed on the ZnCr oxide catalyst was also performed. Both C_7 linear olefins and C_8 dienes were observed to desorb at

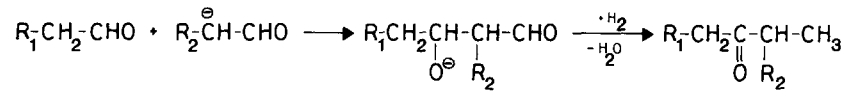

(I)

FIG. 6. Mechanism of aldol-like condensation of aldehydes with oxygen retention reversal. R_1, R_2 = alkyl groups or hydrogen.

the same temperature and with the same distribution seen during *n*-butanal TPSR. This is consistent with the proposed mechanisms, involving either Cannizzaro-type disproportionation or oxidation of the molecularly adsorbed 2-ethyl-2-hexenal to produce C_8 carboxylate and alkoxide surface species.

C_8 intermediate surface species during n-butanoic acid TPSR. The desorption of noticeable amounts of 4-heptanone during *n*-butanoic acid TPSR suggests that ketonization reactions involving carboxylic acids occur to a large extent over ZnCr oxide catalyst. Ketone desorption is likely to occur via decarboxylation of species B_4 in Fig. 5 (route XXV), formed by condensation of two acid molecules with a mechanism similar to that proposed in (*40, 41*) (route XXIII). In addition, a decarboxylative alkyl anion transfer giving rise to species B_5 (*40*) (route XXIV) cannot be ruled out. Both mechanisms involve a molecularly adsorbed acid molecule. However, only very small amounts of 4-heptanone are desorbed during 1-butanol TPSR, although the presence of C_4 carboxylate species on the catalyst surface has been detected. In fact, the oxidative dehydrogenation reaction involving the alkoxide species is likely to lead directly to the carboxylate species, without formation of molecularly adsorbed acid or aldehydic molecules. The TPSR of 1-butanol, when performed with 1-butanol added to the carrier gas (*32*), showed the formation of *n*-butanal and the subsequent desorption of 4-heptanone at T_M = 340°C and T_M = 360°C, respectively. This eventually suggests that the evolution of 4-heptanone during 1-butanol TPSR is prevented by the lack of molecularly adsorbed carbonylic compounds.

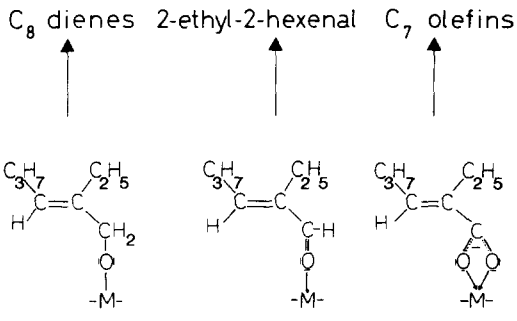

FIG. 7. Intermediate surface species originating from dehydration of species B_2 and corresponding alkoxide and carboxylate species. Symbols as in Fig. 4.

Comparison between C_8 intermediate surface species produced upon adsorption of linear C_4 oxygenated molecules. Inspection of Fig. 5 indicates that different intermediate surface species are involved in the desorption of 4-heptanone. In *n*-butanal TPSR 4-heptanone is produced by decomposition of species B_3 whereas in *n*-butanoic acid TPSR 4-heptanone is produced from species B_4 and/or B_5. The participation of different intermediate surface species is reflected by the different peak temperatures of 4-heptanone desorption in *n*-butanal (T_M = 303°C) and *n*-butanoic acid (T_M = 333°C) TPSR. In addition, C_7 linear olefins were not detected in *n*-butanoic acid TPSR, in contrast to *n*-butanal TPSR. This is easily explained by considering that species B_4 and B_5 cannot be dehydrated, whereas species B_3 can.

The desorption of 4-heptanone occurs both in the low (T_M = 100°C)- and in the high

(T_M = 303°C)-temperature region during *n*-butanal TPSR. Along similar lines Idriss (*42*) reported that the evolution of acetone during TPD of acetaldehyde from Cu/ZnO/Al_2O_3 occurs at different temperatures. Kienneman *et al.* (*43*) invoked the reaction of an acyl species to explain the formation of acetone at low temperature (<160°C) without carbon dioxide evolution following acetaldehyde adsorption over a cobalt–copper catalyst. In fact, no CO_2 has been detected in the low-temperature region during our TPSR experiments. The desorption of 4-heptanone at low temperatures is not observed in *n*-butanoic acid TPSR. One can speculate that, in this case, a particular mechanism involving only aldehyde molecules can be invoked (e.g., decarbonylation of intermediate surface species B_2). Indeed, TPSR experiments performed by coadsorbing *n*-butanal and propanoic acid over a K_2O-promoted ZnCr oxide sample (*44*) indicated the desorption of all the possible expected ketones originating from reaction between aldehyde and acid molecules (namely 4-heptanone, 3-hexanone, and 3-pentanone), but only 4-heptanone was detected in the low-temperature region. This confirms that acid molecules cannot be involved in ketonization reactions at low temperatures, whereas aldehyde molecules can. The same arguments apply in the case of isobutanal TPSR (see Section (b)2). However, both IR data (*32*) and kinetic simulations of TPSR spectra (*44*) indicate that the C_8 carboxylate precursor of 4-heptanone in *n*-butanoic acid TPSR is formed at low temperature, the evolution of 4-heptanone being controlled by its decarboxylative decomposition.

6. *Origin of the Minor Products*

The minor products include methane, ethylene, C_5 hydrocarbons, aromatics (mainly toluene), and 2-pentanone. They are probably formed either by decomposition of heavy surface intermediates or by consecutive reactions of the main desorbed species. In particular, the formation of C_1–C_5 hydrocarbons observed at high temperature is best explained by cracking or by decomposition of carboxylate species. In the case of *n*-butanal TPSR, toluene is possibly produced by dehydrogenation and aromatization of C_7 linear olefins and/or by deoxidation–aromatization of 4-heptanone, along the lines proposed by Idriss (*42*) to account for the formation of propane from acetone. The former route is believed to be of minor relevance during *n*-butanoic acid TPSR, since C_7 linear olefins were not observed in this experiment whereas toluene was still detected. Evolution of C_7 linear olefins during 2-ethyl-2-hexenal TPSR (*44*) was accompanied by desorption of toluene and C_7 dienes, thus suggesting that C_7 linear olefins undergo successive dehydrogenation reactions. The origin of 2-pentanone deserves additional study and is presently under investigation.

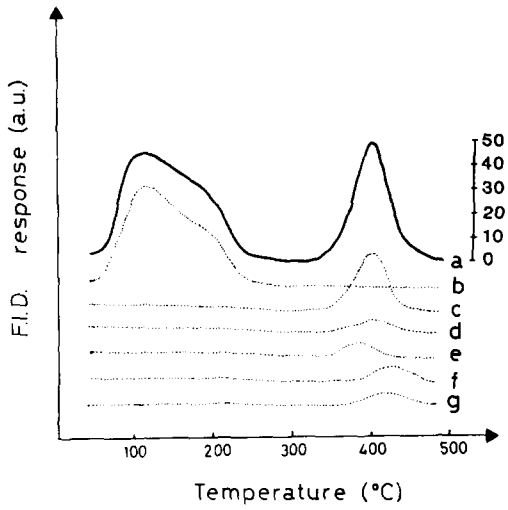

FIG. 8. FID–TPSR traces obtained after isobutanol adsorption at 35°C on ZnCr oxide. (a) Overall FID–TPSR trace; (b) isobutanol; (c) propylene; (d) butenes; (e) aromatics; (f) methane + ethylene; (g) C_5 hydrocarbons.

(b) Adsorption of Branched Oxygenated Molecules on Unpromoted ZnCr Oxide

1. *Isobutanol TPSR on ZnCr Oxide*

Figure 8 shows the TPSR profile obtained after a saturation dose of isobutanol on the

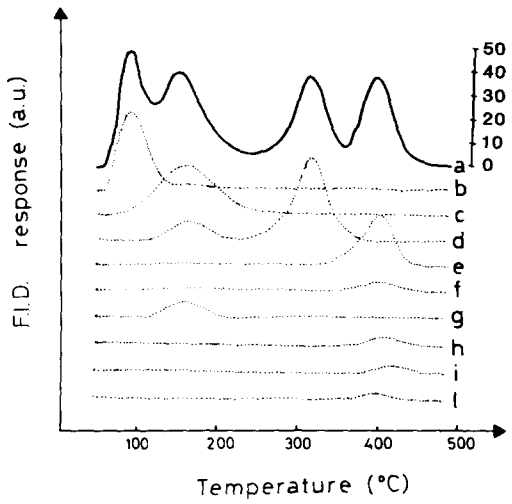

FIG. 9. FID–TPSR traces obtained after isobutanal adsorption at 35°C on ZnCr oxide. (a) Overall FID–TPSR trace; (b) isobutanal; (c) isobutanol (d) diisopropyl ketone; (e) propylene; (f) butenes; (g) unidentified hydrocarbon; (h) aromatics; (i) C_5 hydrocarbons; (l) methane + ethylene.

ZnCr oxide sample. Two main desorption peaks are evident: a low-temperature peak with T_M = 110°C and shoulder at T = 170°C associated with isobutanol desorption, and a high-temperature peak with T_M = 400°C associated with the evolution of propylene and of minor amounts of methane, ethylene, butenes, C_5 hydrocarbons, and aromatics. The use of a TC detector confirmed the presence of CO_2 corresponding with the high-temperature peak.

2. *Isobutanal TPSR on ZnCrO Oxide*

The TPSR spectra obtained after adsorption of isobutanal on ZnCr oxide are shown in Fig. 9. Four maxima are evident in the overall FID–TPSR trace at 83, 150, 310, and 400°C associated primarily with the desorption of: (i) isobutanal; (ii) isobutanol (together with di-isopropyl ketone (2,4-dimethyl-3-pentanone) and a hydrocarbon with a number of carbon atoms ≥8); (iii) diisopropyl ketone; and (iv) propylene, with minor amounts of methane, ethylene, C_5 hydrocarbons, and aromatics. As in the case of isobutanol TPSR, CO_2 was detected corresponding with the high-temperature region. Tables 1 and 2 report the GC–FTIR analysis of the heavier products condensed in a liquid-N_2-cooled CS_2 trap (*29*) in the T ranges 30–250°C and 250–350°C, respectively.

3. *Isobutanoic Acid TPSR on ZnCrO Oxide*

Figure 10 shows the TPSR spectra obtained after adsorption of isobutanoic acid on the ZnCr oxide sample. Isobutanoic acid is desorbed in the low-temperature region, solid particles are formed in the temperature range 220–330°C (which prevented the recording of TPSR traces in this region), and several species (di-isopropyl ketone, propylene, C_1–C_7 hydrocarbons, and an unidentified product whose carbon number is ≥8, as indicated by HRGC analysis) comprise the high-temperature peak. The liquid product condensed between 220 and 330°C mainly consists of isobutanoic acid and diisopropyl ketone. The solid particles, as revealed by IR analysis, appear to be zinc isobutyrate. TCD analysis showed the presence of CO_2 corresponding with the high-temperature peak.

4. *Origin of C_4 Intermediate Surface Species and Desorbed Products*

Figure 4 is appropriate to represent the nature of surface iso-C_4 intermediate species and of the products desorbed therefrom, with $-R = -CH(CH_3)_2$.

Branched intermediate surface species behave similarly to the corresponding linear ones, with only minor differences. In particular, the carboxylate ions are more stable toward decarboxylation, as reflected by the higher temperature of propylene evolution (400°C vs 380°C). The value of the activation energy for decomposition E_d estimated using Eq. (7) for the isocarboxylate ion led to E_d = 46.3 kcal/mol, that is, 1.4 kcal/mol greater than for the *n*-carboxylate ion. Considering that the desorption of propylene in-

TABLE 1

TPSR of Isobutanal on ZnCr Oxide: Analysis of the Products Desorbed in the Range 30–250°C and Condensed in the CS_2 Trap at −196°C

FTIR features	Proposed identification
$\nu_{C-H}(CH_2,CH_3)$ at 2881–2964 cm^{-1}(s) ν_{C-H}(C=O) at 2794(w), 2709(m) cm^{-1} $\nu_{C=O}$ at 1748 cm^{-1} (vs) $\delta_{C-H\ antisym}(CH_3)$ at 1470 cm^{-1} (w) $\delta_{C-H\ sym}(CH_3)$ at 1382 cm^{-1} (w)	Isobutanal
ν_{O-H} at 3672 cm^{-1}(w) $\nu_{C-H}(CH_2,CH_3)$ at 2895–2964 cm^{-1}(s) $\delta_{C-H\ antisym}(CH_3)$ at 1470 cm^{-1}(w) $\delta_{C-H\ sym}$ (CH_3) at 1382 cm^{-1}(w) ν_{C-O} at 1042 cm^{-1}(s)	Isobutanol
$\nu_{C-H}(CH_2,CH_3)$ at 2891–2943 cm^{-1}(s) $\nu_{C=O}$ at 1724 cm^{-1}(s) $\delta_{C-H\ antisym}(CH_3)$ at 1470 cm^{-1}(w) $\delta_{C-H\ sym}(CH_3)$ at 1384 cm^{-1}(w) ν_{C-C}(C—CO—C) at 1021 cm^{-1}(m)	Di-isopropyl ketone
$\nu_{C-H}(CH_2,CH_3)$ at 2880–2968 cm^{-1}(s) $\delta_{C-H\ antisym}(CH_3)$ at 1463 cm^{-1}(w) $\delta_{C-H\ sym}(CH_3)$ at 1384 cm^{-1}(w) ν_{C-C} at 1057 cm^{-1}(w)	Branched hydrocarbon ($N_c \geq 8$)[a]

Note. (vs) very strong; (s) strong; (m) medium; (w) weak.
[a] Determined by HRGC analysis.

volves an H^- extraction from a $-CH_2-$ and from a $-CH_3$ group of the linear or branched carboxylate ion, respectively, the higher E_d observed in the case of the isomolecules can be explained by the lower basicity of the hydrogen of the methyl group.

5. *Origin of C_8 Intermediate Surface Species and Desorbed Products*

C_8 intermediate surface species formed upon isobutanal adsorption on the ZnCr oxide surface differ from the corresponding ones suggested in the case of *n*-butanal adsorption.

No direct evidence for existence of the correspondent of species B_2 on the catalyst surface has been obtained, since no C_8 aldehydes have been detected among the desorbed products.

On the other hand, the desorption of large amounts of di-isopropyl ketone during isobutanal TPSR indicates that the correspondent of species B_3 is present on the surface. This intermediate species (species D_1 of Fig. 11) is formed by condensation of an iso-C_4 carboxylate molecule (which can be formed at room temperature upon aldehyde adsorption on oxidic surfaces (*32*)) with an isobutanal molecule (route XXV), possibly according to the mechanism previously discussed for linear molecules. Decarboxylation of this species (route XXVII) is believed to result in the desorption of di-isopropyl ketone (T_M = 310°C). Unlike in *n*-butanal TPSR, no C_7 olefins have been detected through decarboxylation. This result can be explained considering that the H* hydrogen atom present in the intermediate surface species D_1 of Fig. 11 is sterically hindered by the two neighboring methyl groups and

TABLE 2

TPSR of Isobutanal on ZnCr Oxide: Analysis of the Products Desorbed in the Range 250–350°C and Condensed in the CS_2 Trap at −196°C

FTIR features	Proposed identification
$\nu_{C-H}(CH_2,CH_3)$ at 2915–2979 cm^{-1}(s) $\nu_{C=O}$ at 1727 cm^{-1}(s) $\delta_{C-H\ antisym}(CH_3)$ at 1468 cm^{-1}(w) $\delta_{C-H\ sym}(CH_3)$ at 1381–1354 cm^{-1}(w) ν_{C-C}(C—CO—C) at 1105 cm^{-1}(w)	C_7 Ketone
$\nu_{C-H}(CH_2,CH_3)$ at 2891–2943 cm^{-1}(s) $\nu_{C=O}$ at 1724 cm^{-1}(s) $\delta_{C-H\ antisym}(CH_3)$ at 1470 cm^{-1}(w) $\delta_{C-H\ sym}(CH_3)$ at 1384 cm^{-1}(w) ν_{C-C}(C—CO—C) at 1021 cm^{-1}(m)	Di-isopropyl ketone
$\nu_{C-H}(=CH_2)$ at 3100 cm^{-1}(w) $\nu_{C-H}(CH_2,CH_3)$ at 2885–2977 cm^{-1}(s) $\nu_{C=O}$ at 1724 cm^{-1}(vs) $\nu_{C=C}$ at 1627 cm^{-1}(w) $\delta_{C-H\ antisym}(CH_3)$ at 1459 cm^{-1}(m) $_{C-H\ sym}(CH_3)$ at 1382 cm^{-1}(m) sorbance at 1280 cm^{-1}(w) $_{-C}$(C—CO—C) at 1046 cm^{-1}(s) .sorbance at 988 cm^{-1}(w) $\gamma_{C-H}(=CH_2)$ at 922 cm^{-1}(m)	C_7 Unsaturated ketone
$\nu_{C-H}(CH_2,CH_3)$ at 2888–2974 cm^{-1}(s) $\nu_{C=O}$ at 1724 cm^{-1}(s) $\delta_{C-H\ antisym}(CH_3)$ at 1467 cm^{-1}(m) $\delta_{C-H\ sym}(CH_3)$ at 1381–1361 cm^{-1}(w) ν_{C-C}(C—CO—C,C—C) at 1115 cm^{-1}(w), 1023 cm^{-1}(w)	C_7 Ketone

Note. (vs) very strong; (s) strong; (m) medium; (w) weak.

is not acidic enough to be involved in dehydration. Accordingly the decomposition of species D_1 produces only di-isopropyl ketone and not branched C_7 olefins.

The desorption of di-isopropyl ketone in isobutanoic acid TPSR provides evidence for the presence of the intermediate surface species D_2 depicted in Fig. 11. Indeed, decarboxylation and keto-enol tautomerism of species D_2 (route XXVIII) eventually results in the evolution of di-isopropyl ketone. The presence of solid particles in the gas phase during isobutanoic acid TPSR, as previously reported (see Section (b)3), made the accurate determination of the di-isopropyl ketone peak temperature difficult. However, it appears that, as in the case of linear molecules, C_7 ketone desorption during aldehyde TPSR occurs at slightly lower temperatures as compared to acid TPSR. Species D_2 is formed via condensation of two isobutanoic acid molecules followed by dehydration (route XXVI), according to a mechanism similar to that suggested for *n*-butanoic acid, and corresponds to species B_4 in Fig. 5. The small amounts of di-isopropyl ketone detected during isobutanoic acid TPSR as compared to 4-heptanone during *n*-butanoic acid TPSR are explained by the slow rate of the dehydration step, which also accounts for the absence of C_7 branched olefins.

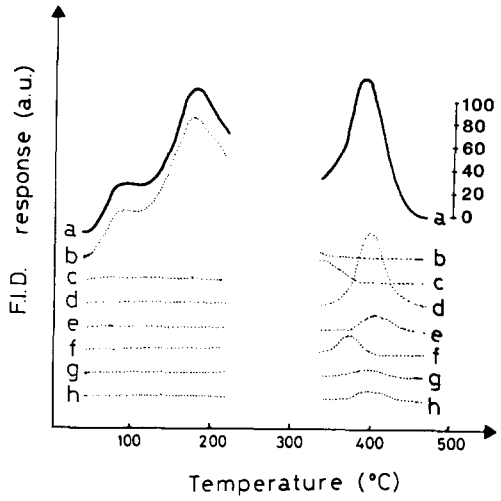

FIG. 10. FID–TPSR traces obtained after isobutanoic acid adsorption at 35°C on ZnCr oxide. (a) Overall FID–TPSR trace; (b) isobutanoic acid; (c) di-isopropyl ketone; (d) propylene; (e) aromatics; (f) unidentified species; (g) butenes; (h) C_5 hydrocarbons.

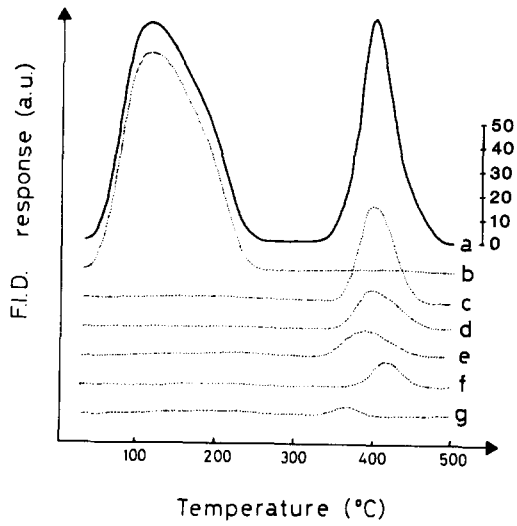

FIG. 12. FID–TPSR traces obtained after 1-butanol adsorption at 35°C on the K-doped ZnCr oxide. (a) Overall FID–TPSR trace; (b) 1-butanol; (c) propylene; (d) aromatics; (e) C_5 hydrocarbons; (f) methane + ethylene; (g) 4-heptanone.

(c) Adsorption of Linear C_4 Oxygenated Molecules on Potassium-Promoted ZnCr Oxide

Previous results point to a lower reactivity of iso-molecules with respect to the corresponding linear ones. Accordingly, linear C_4 oxygenated compounds have been selected for a TPSR investigation on the effects of alkali addition to the ZnCr oxide system.

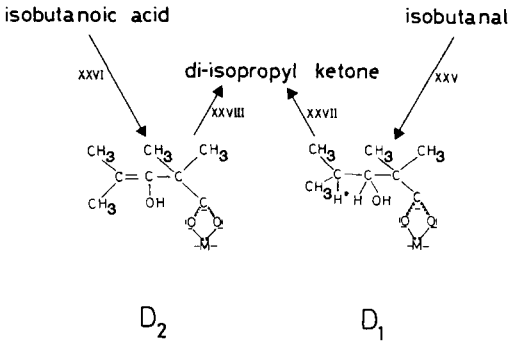

FIG. 11. C_8 proposed intermediate surface species formed upon isobutanal and isobutanoic acid adsorption on ZnCr oxide and products desorbed thereform. Symbols as in Fig. 4.

1. 1-Butanol TPSR on ZnCr Oxide + K_2O

The TPSR traces obtained after 1-butanol adsorption are shown in Fig. 12. Two main peaks are evident: a low-temperature peak associated with 1-butanol evolution (T_M = 110°C), and a high-temperature peak associated with the desorption of propylene (T_M = 400°C) + CO_2 (monitored by TCD), and of minor amounts of methane, ethylene, butenes, C_5 hydrocarbons, aromatics, and 4-heptanone. Experiments performed in a different TPSR apparatus equipped with a quadrupole UTI 100C mass spectrometer for on-line analysis of the desorbed products confirmed the results of Fig. 12 and further showed two H_2 desorption peaks with $T_M \approx 220$ and 400°C. The two peaks are probably associated with the oxidative dehydrogenation of butoxy to butoxylate species (reaction (8) and/or reaction (9)):

$$CH_3CH_2CH_2CH_2O_{(a)} + O_{(s)} \rightarrow CH_3CH_2CH_2COO_{(a)} + H_2 \quad (8)$$

$$CH_3CH_2CH_2CH_2O_{(a)} + OH_{(a)}$$

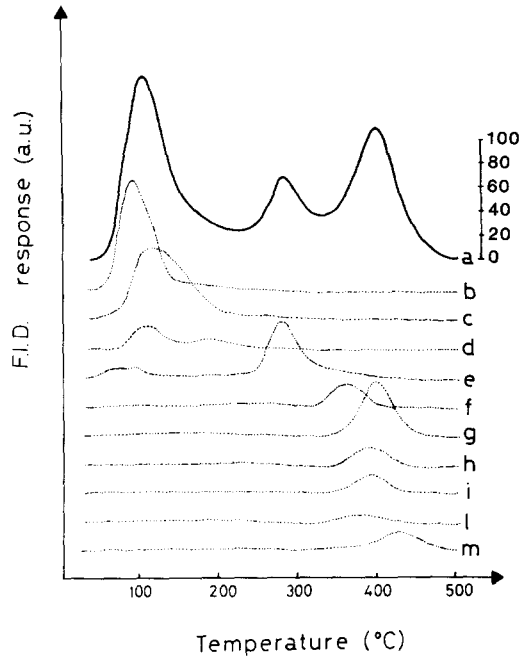

FIG. 13. FID–TPSR traces obtained after *n*-butanal adsorption at 35°C on the K-doped ZnCr oxide. (a) Overall FID–TPSR trace; (b) *n*-butanal; (c) 2-ethyl-2-hexenal; (d) 1-butanol; (e) 4-heptanone; (f) C_7 linear olefins; (g) propylene; (h) toluene; (i) C_5 hydrocarbons; (l) butenes; (m) methane + ethylene.

$$\rightarrow CH_3CH_2CH_2COO_{(a)} + 3/2\ H_2 \quad (9)$$

and to the dehydrogenation–decarboxylation of butoxylate species leading to propylene (reaction (6)), respectively.

2. *n-Butanal TPSR on ZnCr Oxide + K_2O*

Three main peaks are evident in the overall FID–TPSR trace obtained upon *n*-butanal saturation on the sample (Fig. 13). The first peak is associated with the evolution of *n*-butanal, 2-ethyl-2-hexenal, 1-butanol, and 4-heptanone; the second peak with T_M = 280°C is primarily caused by the desorption of 4-heptanone and, to a lesser extent, of C_8 ketones (not reported in the figure); and the third peak with T_M = 400°C corresponds to the evolution of C_7 linear olefins, propylene, toluene, C_5 hydrocarbons, butenes, methane, and ethylene. TC data showed CO_2 corresponding with the high-temperature region.

3. *n-Butanoic Acid TPSR on ZnCr Oxide + K_2O*

n-Butanoic acid TPSR on the alkali-doped ZnCr oxide sample (Fig. 14) results in a low-temperature desorption peak closely resembling that observed on the unpromoted ZnCr oxide (see Fig. 3). Much more pronounced were the peak with T_M = 355°C, associated with 4-heptanone desorption, and the shoulder at ≈400°C, associated with propylene evolution. Also monitored in the high temperature region were 2-pentanone and toluene, along with CO_2 detected by TCD. Contrary to *n*-butanoic acid TPSR on the unpromoted sample, the formation of solid particles was not observed.

The FID–TPSR traces of *n*-butanoic acid obtained with different initial coverages of the adsorbate are shown in Fig. 15. It is apparent that by lowering the initial coverage the desorption of 4-heptanone is affected markedly whereas the amount of propylene evolved decreases only at very low coverages. This indicates that C_4 carboxyl-

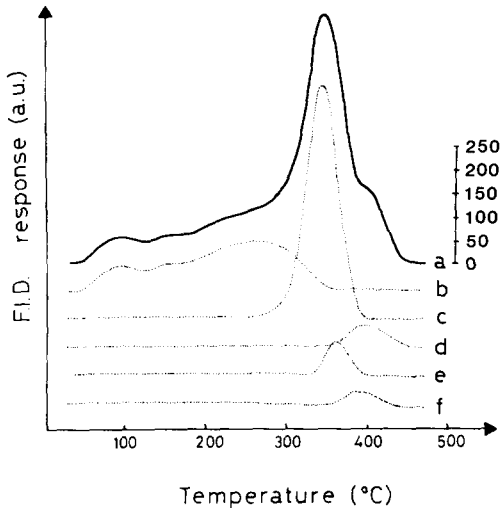

FIG. 14. FID–TPSR traces obtained after *n*-butanoic acid adsorption at 35°C on the K-doped ZnCr oxide. (a) Overall FID–TPSR trace; (b) *n*-butanoic acid, (c) 4-heptanone, (d) propylene; (e) 2-pentanone; (f) toluene.

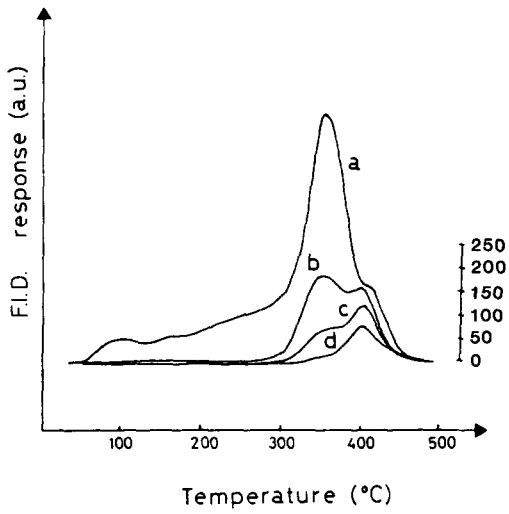

FIG. 15. FID–TPSR traces obtained after different initial coverage of *n*-butanoic acid on the K-doped ZnCr oxide. (a) saturation coverage; (b) $\frac{1}{2}$ saturation coverage; (c) $\frac{1}{4}$ saturation coverage; (d) $\frac{1}{8}$ saturation coverage.

ate species, leading to propylene + CO_2, are formed at the strongest surface sites, whereas C_8 carboxylate species which give rise to 4-heptanone are produced only after saturation of these sites. Moreover, the peak temperature of 4-heptanone, like that of propylene, does not depend on the initial coverage, which indicates that the desorption of 4-heptanone is controlled by decomposition of its adsorbed precursor (first-order decomposition kinetics).

(d) Catalytic Functions of the Unpromoted and K-Promoted ZnCr Oxide and their Relevance under HAS Conditions

1. Aldol condensation reactions occur over ZnCr oxide according to both the "normal" mode, as reflected by the formation of 2-ethyl-2-hexenal during *n*-butanal TPSR, and to the "oxygen retention reversal" mode, as indicated by the formation of C_8 ketones. Aldol condensations of branched molecules do not occur, since no C_8 aldehydes were detected during isobutanal TPSR.

No significant effects of alkali addition were apparent on aldol condensations, based on the amounts of 2-ethyl-2-hexenal-desorbed during *n*-butanal TPSR. Indeed, it appears that the presence of alkali metal ions is not essential to catalyze this class of reactions.

Thus, the TPSR data support the mechanism for chain growth during HAS based on crossed condensations of aldehydes (*26, 3*), which however do not take place on >CH– groups (*27*), making β-branched oxygenates the terminal species of the chain growth mechanism and therefore the most abundant products, as actually observed. Furthermore, aldol condensations with oxygen retention reversal are involved in ketone production under HAS as well (*21*).

Notably, aldol condensations both in the "normal" and in the "oxygen retention reversal" mode have been observed also in continuous flow microreactor experiments at atmospheric pressure in the temperature range 360–405°C over the same K-promoted catalyst as used in this work (*45*).

2. Ketonization reactions, involving both linear and branched molecules, were also apparent under TPSR conditions. Our results are consistent with proposed mechanisms (*21, 40, 41*) which invoke a reaction between a carboxylate species and an aldehyde or acid molecule. As discussed below, carboxylate species are involved also in decarboxylation reactions leading to olefins. Ketonization reactions were greatly promoted by the addition of alkali metal ions to the catalyst: during both *n*-butanal and *n*-butanoic acid TPSR the amount of desorbed 4-heptanone was markedly enhanced. However, the influence on T_M is the opposite: T_M was shifted from 303°C down to 280°C in *n*-butanal TPSR and from 333°C up to 350°C in *n*-butanoic acid TPSR. This is consistent with the fact that different combinations of catalyst functions are involved in the desorption of 4-heptanone starting from precursors B_3 (dehydrogenation + decarboxylation + ketoenol tautomerism) and B_4 (decarboxylation + ketoenol tautomerism), so that different rate-limiting steps are in-

volved in the decomposition kinetics of the above species.

Although large quantities of 4-heptanone and di-isopropyl ketone were formed during TPSR of linear and branched C_4 oxygenates, ketones are typically only minor products of HAS over modified high-temperature methanol catalysts (<2–3% w/w of the liquid products). The apparent contradiction is solved by considering that a strong ketonization reactivity is effective also under typical synthesis conditions, but chemical equilibrium is approached between ketones and primary alcohols according to the stoichiometry (*46*).

$$R_1CH_2OH + R_2CH_2OH \rightleftharpoons R_1—CO—R_2 + CO + 3H_2 \quad (10)$$

In fact, the small content of ketones in the HAS product mixture at moderate to high pressures is consistent with the unfavorable inverse cubic dependence of their equilibrium concentrations on the total pressure. The departures from thermodynamic equilibrium observed at low temperatures and short contact times further suggest that reaction (10) is associated with the consumption of ketones rather than with their formation (*46*). Therefore an alternative route leading directly to the formation of ketones should exist during HAS: this probably involves aldol-type condensations with oxygen retention reversal, as previously discussed.

3. Decarboxylation was one of the most evident functions of the ZnCr oxide system indicated by TPSR experiments with 1-butanol and *n*-butanal (*28, 29*). TPSR of linear and branched acid molecules, together with IR, have provided direct evidence that olefins originate under TPSR conditions mainly from decomposition of carboxylate species. The present study further indicates that isocarboxylate species are more stable toward decarboxylative decomposition than the corresponding linear ones.

Decarboxylation of *n*-butyrate ion to propylene and CO_2 occurs to a lesser extent over the K-promoted ZnCr oxide catalyst, as reflected by the lower amount of desorbed propylene, and at a higher temperature (400 vs 380°C). Such results agree with the results of a previous TPD study of isopropanol on an alkali-doped ZnO catalyst (*38*), and with the greater stability of basic carboxylate species.

The decarboxylation function revealed by TPSR may play a role in the undesired formation of hydrocarbons during HAS over similar catalysts. Notably, the adverse influence of alkali promotion on the decarboxylation function parallels the decrease in the selectivity to olefins and hydrocarbons observed in HAS upon adding K- or Cs-metal ions to ZnCr oxide catalysts (*11*).

4. The observed formation of carboxylate species following adsorption of linear alcohol and aldehyde molecules, as well as the desorption of C_7 ketones, requires a dehydrogenation function. The results of isobutanol, isobutanal, and isobutanoic acid TPSR confirm that this dehydrogenation function is effective also with branched molecules, while detection of aromatics (toluene) among the products of TPSR over K-doped ZnCr oxide, along with the formation of 4-heptanone and propylene, indicates that the dehydrogenation reactivity is still effective after the addition of potassium.

A complementary hydrogenation function of the ZnCr oxide system had been previously inferred from the desorption of 1-butanol and butenes during *n*-butanal TPSR (*29*): it is confirmed in the present study by the evolution of isobutanol and butenes during isobutanal TPSR. As already suggested for the case of 1-butanol and confirmed by IR, a disproportionation reaction of isobutanal leading to isobutanol and isobutanoic acid is likely to operate at low temperatures.

The hydrogenation–dehydrogenation functions revealed by the TPSR study are quite effective under HAS conditions as indicated by the close approach to chemical equilibrium between aldehydes and primary alcohols and between ketones and second-

ary alcohols (*46, 47*). It is worth noting, however, that chemical equilibrium is not approached in the hydrogenation of olefins to the corresponding paraffins (*9*).

5. The formation of C_7 linear olefins, C_8 dienes, and butene observed during *n*-butanal TPSR involves a dehydration step (*29*). Furthermore, the formation of 2-ethyl-2-hexenal from intermediate surface species B_2 during *n*-butanal TPSR requires a dehydration function. During isobutanal TPSR, butenes, but no C_7 linear olefins and C_8 dienes, were observed, due to the different reactivity of this molecule. Therefore, the dehydration function is confirmed, although less evident, by the TPSR of branched oxygenated molecules.

Upon addition of potassium to the catalyst, C_8 dienes were no longer detected, and a reduction in the formation of butenes and C_7 linear olefins was noted. Thus, alkali promotion of ZnCr oxide significantly depressed the dehydration function.

Like decarboxylation, dehydration may be partially responsible for the formation of hydrocarbons during HAS. Indeed, one of the most relevant effects brought about by addition of alkali metal ions under real synthesis conditions is the decrease of the dehydration function of unpromoted ZnCr oxide, as evidenced in the lower productivity to ethers (*11, 27*).

6. The TPSR study showed the presence of a hydrolysis function on both the unpromoted and K-promoted catalyst which is exploited in the desorption of isobutanol from isobutoxy intermediate, and is in line with previous indications collected during *n*-butanal and 1-butanol TPSR (*28, 29*). A similar function, namely alcoholysis, can be invoked to explain the formation of ethers from alkoxide species and of methyl esters from carboxylate species in HAS. It is worth noting that the esterification route appears to be suitable for the generation of both methyl formate and higher methyl esters (as opposed to the carbonylation of alkoxide species which can explain the formation of methyl formate but not of higher methyl esters), and is also consistent with the prevailing thermodynamic constraints on the concentrations of methyl esters (*46*).

7. As already discussed, the migration of the C=C double bond is responsible for a number of isomers of both olefins and oxygenated unsaturated compounds during *n*-butanal TPSR (*29*). In addition, keto enol tautomerism is involved in the desorption of 4-heptanone, di-isopropyl ketone, and C_8 ketones. The isomerization function operates over both unpromoted and alkali-promoted ZnCr oxide.

CONCLUSIONS

A number of characteristic chemical functions of the unpromoted ZnCr oxide catalyst have been identified by the TPSR study, namely aldol-like condensation (also with oxygen retention reversal), decarboxylation and decarboxylative condensation, hydrogenation–dehydrogenation, dehydration, and hydrolysis along with isomerization and cracking. Alkali addition results in lowering the dehydration and decarboxylation functions, enhances the functions responsible for the formation of C_7 ketones, and apparently has no significant effect on aldolic condensation reactions leading to aldehydes. Such results are in line with the variations observed in the HAS product distribution changing from the unpromoted to the alkali-promoted catalyst. On comparing these data with information obtained by catalytic tests performed under real synthesis conditions and by thermodynamic analysis, a strict correspondence is noted between the characteristic chemical functions indicated by the TPSR analysis and those operating during HAS. However, in the synthesis some of the associated chemical reactions are limited by chemical equilibrium so that the concentrations of related compounds are eventually very small. This is the case of condensation–decarboxylation reactions leading to ketones and of hydrogenations of aldehydes and ketones to the corresponding alcohols.

The TPSR technique has also provided direct information on the surface reaction

mechanisms involved in the alcohol chain growth and in the formation of other minor products, such as ketones, secondary alcohols, and hydrocarbons. In particular, the mechanism of chain growth leading to C_{3+} primary alcohols involves a series of crossed aldolic condensations of aldehydic molecules. Such a mechanism is effective on both unpromoted and K_2O-doped ZnCr oxide catalyst. Comparison of *n*-butanal and isobutanal TPSR data reveals that branched oxygenates behave as terminal species in the alcohol chain growth, which explains the abundance of isobutanol in the reaction mixture.

Condensation reactions followed by decarboxylation are also involved in the evolution of ketones. This mechanism operates on both linear and branched molecules, as well as on aldehydic and acid molecules, and is markedly enhanced by alkali addition. Formation of ketones occurs also by aldol-like condensations with oxygen retention reversal. Under typical HAS conditions, both mechanisms are effective; however, the former route is associated with the consumption of ketones due to different operating conditions, whereas the latter route is responsible for their formation. Thermodynamics dictate low equilibrium concentrations of ketones at high pressures: this eventually accounts for the small amounts of ketones detected in the product mixture obtained over alkali-promoted high-temperature methanol catalysts.

TPSR and IR have confirmed the crucial role played by carboxylate species in the formation of olefins via decarboxylation reactions, which represents a possible route for the origin of hydrocarbons in the synthesis. Carboxylate species are also involved in ketonization reactions and in the formation of methyl esters.

Formation of hydrocarbons occurs also by dehydration of alcohols.

The lower reactivity of branched compounds toward decarboxylation and dehydration indicates that such species are far less involved in successive reactions as compared to linear compounds, in line with their terminal character in HAS.

ACKNOWLEDGMENTS

Financial support from CNR/Progetto Finalizzato Energetica 2 is gratefully acknowledged. The authors thank Professors E. Mantica and D. Botta for assistance in GC–FTIR measurements, Professor L. Forni for assistance during TPD–MS measurements with a quadrupole mass spectrometer, and Professor G. Busca and Dr. N. Ferlazzo for useful discussion.

REFERENCES

1. Smith, K. J., and Anderson, R. B., *Canad. J. Chem. Eng.* **61,** 40 (1983).
2. Klier, K., *in* "Catalysis on the Energy Scene" (S. Kaliaguine and A. Mahay, Eds.), p. 439. Elsevier, Amsterdam, 1984.
3. Vedage, G. A., Himelfarb, P. B.,Simmons, G. W., and Klier, K., *ACS Symp. Ser.* **279,** 295 (1985).
4. Fornasari, F., Gusi, S., La Torretta, T. M. G., Trifirò, F., and Vaccari, A., *in* "Catalysis and Automotive Pollution Control" (A. Crucq and A. Frennet, Eds.), p. 469. Elsevier, Amsterdam, 1987.
5. Anderson, R. B., Feldman, J. B., and Storch, H. H., *Ind. Eng. Chem.* **44,** 2418 (1952).
6. Runge, F., and Zepf, K., *Brennst. Chem.* **35,** 167 (1954).
7. Natta, G., Colombo, U., and Pasquon, I., *in* "Catalysis" (P. H. Emmett, Ed.), Vol. 5. Reinhold, New York, 1957.
8. Riva, A., Trifirò, F., Vaccari, A., Busca, G., Mintchev, L., Sanfilippo, D., and Manzatti, W., *J. Chem. Soc. Faraday Trans. 1* **83,** 2213 (1987).
9. Tronconi, E., Ferlazzo, N., Forzatti, P., and Pasquon, I., *Ind. Eng. Chem. Res.* **26,** 2122 (1987).
10. Forzatti, P., Cristiani, C., Ferlazzo, N. Lietti, L., Pasquon, I., Tronconi, E., Villa, P. L., Antonelli, G. B., Sanfilippo, D., and Contarini, S., *in* "Actas 11th Iberoamerican Symposium on Catalysis," (F. Cossio, O. Bermúdez, G. Del Angel, and R. Gomez, Eds.) Vol. II, p. 671. Guanajuato, Mexico, 1988.
11. Tronconi, E., Lietti, L., Forzatti, P., and Pasquon, I., *Appl. Catal.* **47,** 317 (1989).
12. Forzatti, P., Cristiani, C., Ferlazzo, N., Lietti, L., Tronconi, E., Villa, P. L., and Pasquon, I., *J. Catal.* **111,** 120 (1988).
13. Sugier, A., and Freund, E., U.S. Patent 4122110, 1978.
14. Courty, P., Durand, D., Freund, E., and Sugier, S., *J. Mol. Catal.* **17,** 241 (1987).
15. Nunan, J. G., Bogdan, C. E., Klier, K., Smith, K. J., Young, C. W., Herman, R. G., *J. Catal.* **116,** 195 (1989).
16. Nunan, J. G., Bogdan, C. E., Klier, K., Smith, K. J., Young, C. W., and Herman, R. G., *J. Catal.* **113,** 410 (1988).

17. Smith, K. J., Herman, R. G., and Klier, K., *Chem. Eng. Sci.* **45,** 2639, (1990).
18. Klier, K., Herman, R. G., Nunan, J. G., Smith, K. J., Bogdan, C. E., Young, C. W., Sebastian, J. G., *in* "Methane Conversion" (D. M. Bibby, C. D. Chang, R. F. Howe, and S. Yurchok, Eds.), p. 109. Elsevier, Amsterdam, 1988.
19. Elliott, D. J., and Pennella, F., *J. Catal.* **114,** 90 (1988).
20. Elliott, D. J., *J. Catal.* **111,** 445 (1988).
21. Elliott, D. J., and Pennella, F., *J. Catal.* **119,** 359 (1989).
22. Elliott, D. J., and Pennella, F., *J. Catal.*, **102,** 464 (1986).
23. Frolich, K., and Cryder, S., *Ind. Eng. Chem.* **23,** 1051 (1930).
24. Graves, G. D., *Ind. Eng. Chem.* **23,** 1381 (1931).
25. Morgan, G. T., *Proc. Roy. Soc. A* **127,** 246 (1930).
26. Morgan, G. T., Douglas, D. V. N., and Proctor, R. A., *J. Soc. Chem. Ind. (London)* **41,** 1T (1932).
27. Tronconi, E., Forzatti, P., Groppi, G., Lietti, L., Sanfilippo, D., *in* "Recent Advances in Chemical Engineering" (D. N. Sanef, and D. Kunzru, Eds.), p. 217. Tata-McGraw Hill, New Delhi, India, 1989.
28. Lietti, L., Tronconi, E., and Forzatti, P., *J. Mol. Catal.* **44,** 201 (1988).
29. Lietti, L., Botta, D., Forzatti, P., Mantica, E., Tronconi, E., and Pasquon, I., *J. Catal.* **111,** 360 (1988).
30. Vohs, J. M., and Barteau, M. A., *J. Catal.* **113,** 497 (1988).
31. Vohs, J. M., and Barteau, M. A., *Surf. Sci.* **201,** 481 (1988).
32. Lietti, L., Tronconi, E., Forzatti, P., and Busca, G., *in J. Mol. Catal.*, **55,** 43 (1989).
33. Bowker, M., Petts, R. W., and Waugh, K. C., *J. Catal.* **99,** 53 (1986).
34. Groff, R. P., *J. Catal.* **79,** 259 (1983).
35. Bowker, M., Houghton, H., and Waugh, K. C., *J. Catal.* **79,** 431 (1983).
36. Bowker, M., Houghton, H., and Waugh, K. C., *J. Chem. Soc. Faraday Trans. 1* **77,** 3023 (1981).
37. Takezawa, N., Hanamaki, C., and Kobayashi, H., *J. Catal.* **38,** 101 (1975).
38. Chadwick, D., and O'Malley, P. J. R., *J. Chem. Soc. Faraday Trans 1* **83,** 2227 (1987).
39. Forzatti, P., Tronconi, E., Lietti, L., *in* "Handbook of Heat and Mass Transfer" (N. Cheremisinoff, Ed.), Vol. 3, Chap. 8, p. 299. Gulf Pub. Houston, 1988.
40. Jayamani, M., and Pillai, C. N., *J. Catal.* **87,** 93 (1984).
41. Gonzalez, F., Munuera, G., and Prieto, J. A., *J. Chem. Soc. Faraday Trans. 1* **74,** 1517 (1978).
42. Idriss, H., Ph.D. Thesis, Université Louis Pasteur de Strasbourg, 1987.
43. Kienneman, A., Diagne, C., Hindermann, J. P., Chaumette, P., and Courty, P., *Appl. Catal.* **53,** 197 (1989).
44. Unpublished results from our laboratories.
45. L. Lietti, E. Tronconi, and P. Forzatti, in preparation.
46. Tronconi, E., Forzatti, P., and Pasquon, I., *J. Catal.*, **124,** 376 (1990).
47. Tronconi, E., and Forzatti, P., *Chim. Ind. (Milan)* **70,** 66 (1988).